

Fatigue Crack Growth Mechanisms in a Forged IN 718 Nickel-Based Superalloy

C. Mercer and W. O. Soboyejo

Department of Materials Science and Engineering, The Ohio State University, 2041 College Road, Columbus, OH 43210.

Abstract

The results of an investigation of the mechanisms of fatigue crack propagation in a forged IN 718 nickel-based superalloy are reported. Fatigue deformation and fracture mechanisms are evaluated using transmission electron microscopy analysis of crack-tip regions and scanning electron microscopy studies of fracture surfaces. The effects of increasing stress intensity factor range on fatigue crack growth rates and fracture mechanisms are elucidated. The results presented are in good agreement with similar studies into the fatigue crack propagation behavior of both polycrystalline and single crystal nickel-based superalloys.

1. Introduction

The fatigue properties of nickel-based superalloys has been the focus of a considerable amount of research, [1-9]. Several studies of the mechanisms of fatigue and particularly the dislocation configurations that arise during low and high cycle fatigue of nickel and its alloys have been carried out, [4-8]. However, these investigations are largely concerned with dislocation activity that is associated with the mechanisms of fatigue crack *initiation*. Very little work appears to have been performed concerning the micromechanisms of crack-tip deformation and fracture during fatigue crack *propagation*.

The purpose of this work, therefore, is to investigate the micromechanisms of fatigue crack propagation in forged IN 718, a typical polycrystalline nickel-based superalloy used for turbine disc applications in the aerospace industry. The results of fatigue crack growth experiments are presented. Micromechanisms of crack-tip deformation and cyclic fracture (fatigue crack growth) are proposed based on scanning electron microscopy studies of fracture surfaces and crack-tip transmission electron microscopy examination.

2. Experimental Procedure

The IN 718 forging that was employed in this study was supplied by Wyman Gordon, Houston, TX, in the form of a 5.5 mm thick plate. The plate was cut from a triple melted, (vacuum induction melting + vacuum arc remelting + electroslag remelting), fine-grained billet supplied by Special Metals Corporation, New Hartford, NY. The actual chemical composition of the forging is given in Table I.

Single-edged notched (SEN) specimens were machined from the plate using electro-discharge machining (EDM) techniques. Metallographic analysis was carried out on one of the specimens following polishing and electrolytic etching in oxalic acid solution for approximately 30 seconds using a 6 V D. C. power supply.

Constant load, fatigue crack growth experiments were then carried out under computer control at room temperature. The tests were performed on the SEN specimens under three-point bend loading using a test frequency of 10 Hz and a stress ratio of 0.1. Fatigue crack growth rates (da/dN), and corresponding values of stress intensity factor ranges (ΔK), were calculated using standard expressions provided in the ASTM E 647 code. Crack length was measured using the potential drop technique. Initial stress intensity factor ranges of 15

MPa√m were employed. The fatigue tests were stopped prior to specimen failure. Some specimens were stopped at ΔK values corresponding to the near-threshold regime while others were stopped in the Paris or steady state crack growth regime of the da/dN versus ΔK fatigue crack growth curve [10]. The tests were stopped to enable a detailed examination of the crack-tip region corresponding to each regime using transmission electron microscopy (TEM). Foils were taken perpendicular to the crack front and prepared using a combination of precision dimpling and ion milling techniques to produce an electron transparent region in the foil that was located within the plastic zone directly ahead of the crack-tip. This operation proved to be very difficult and time consuming. The width of the plastic zone, r_p , was estimated using the following expression :-

$$r_p = (1/\pi) (\Delta K/2\sigma_y)^2 \quad (1)$$

where ΔK is the final stress intensity factor range just prior to stopping the test and σ_y is the yield stress.

Foils were also taken from undeformed material well away from the fatigue crack and prepared using the same dimpling and ion milling methods. Comparison of the deformed and undeformed material was then carried out in the TEM so that an attempt could be made to identify the mechanism(s) of fatigue crack growth in this alloy.

Table I. Chemical Composition of IN 718 Forging

Element	Weight %
Ni	54.03
C	0.024
Mn	0.08
Si	0.08
Cr	17.99
Co	0.30
Fe	17.55
Mo	2.96
Nb	5.35
Ti	0.940
Al	0.49
B	0.0027
S	0.0002
P	0.008
Cu	0.03
Ta	0.01
O	6 ppm
N	64 ppm
Mg	21 ppm

Following TEM specimen preparation, the remaining portion of the specimens were fractured under monotonic loading to allow analysis of the fracture surfaces using scanning electron microscopy (SEM). Fracture surfaces that corresponded to the Paris and high ΔK regimes of the fatigue crack growth curve were examined to determine the fracture modes that occur in the near-threshold and Paris regimes.

3. Results and Discussion

(i) Microstructure

A typical optical micrograph of the IN 718 alloy is shown in Fig. 1. The microstructure consists of approximately equi-axed grains of the nickel-rich f.c.c. solid solution (γ phase) with an average grain size of $30\ \mu\text{m}$. Contained within these grains is a moderate density of elongated or lenticular Ni_3Nb precipitates (γ' phase) [11]. The orientations of these γ' precipitates within the matrix material appeared to be somewhat irregular.



Figure 1. Optical micrograph showing general microstructure of forged IN 718 alloy.

The TEM micrographs of the undeformed substructure are given in Fig. 2. The micrographs show a deformation-free substructure with a very low dislocation density, typical of an annealed microstructure. The elongated γ' particles can be clearly seen and these also show no observable deformation.

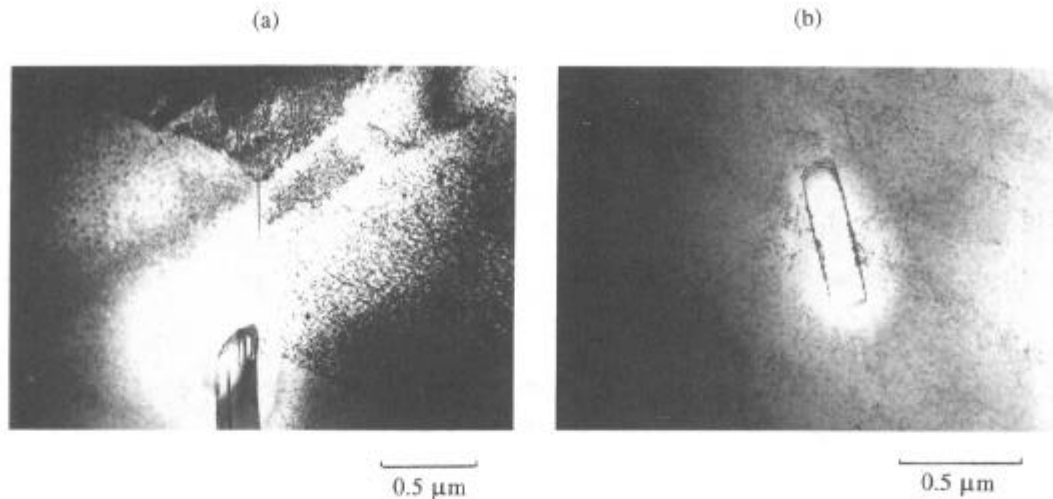


Figure 2. Transmission electron micrographs showing (a) general undeformed substructure and (b) detail of undeformed γ' precipitate.

(ii) Fatigue Crack Growth Rates

The da/dN versus ΔK fatigue crack growth curve obtained for this alloy is presented in Fig. 3. The plot clearly shows the near-threshold regime, the Paris regimes of the curve. Stable crack growth was observed up to a ΔK of $25 \text{ MPa}\sqrt{\text{m}}$ and the data is in good agreement with other studies of similar alloys [1, 9]. The Paris exponent calculated from the curve was 2.98.

The TEM and SEM analysis was carried out on specimens where fatigue testing was halted at ΔK values of approximately 13 and $25 \text{ MPa}\sqrt{\text{m}}$, which correspond to the near-threshold and Paris regimes, respectively.

(iii) Fracture Modes

Typical fatigue fracture surfaces corresponding to the near-threshold and Paris regimes of this alloy are shown in Figs. 4 (a) and 4 (b), respectively. The mode of fracture under cyclic loading in both regimes appeared to be a transgranular, crystallographic mode, as can be seen by the sharp, angular facets in the fracture surfaces, as shown in Fig. 4. No evidence of striation formation or plasticity was observed. Although a crystallographic fracture mode is often observed in the near-threshold regime of metallic materials, it is somewhat unusual for a ductile metal to exhibit this mode of fracture in the Paris or steady state crack growth regime. Such behavior is generally more typical of more brittle materials. However, work by

Lerch and Antolovich [9] have also observed crystallographic fracture occurring up to similar ΔK levels in the single crystal nickel-based superalloy RENÉ N4. A possible explanation for this behavior is that even in the Paris regime, stress intensity levels are still significantly below the fracture toughness of this type of material and so the material fractures in a mode generally associated with low stress intensity values without the occurrence of significant plastic deformation. The tensile overload region of the fracture surface is shown in Fig. 4 (c) for comparison and exhibits the classic ductile-dimple mechanism that would be expected in this type of material.

The only noticeable difference between the fracture surfaces corresponding to the near-threshold and Paris regimes is that a relatively high incidence of secondary cracking was observed in the Paris regime as shown in Fig. 4 (b). The reason for this may be the increased incidence of fracture in crystallographic directions other than the favored crack growth direction at higher stress intensity levels.

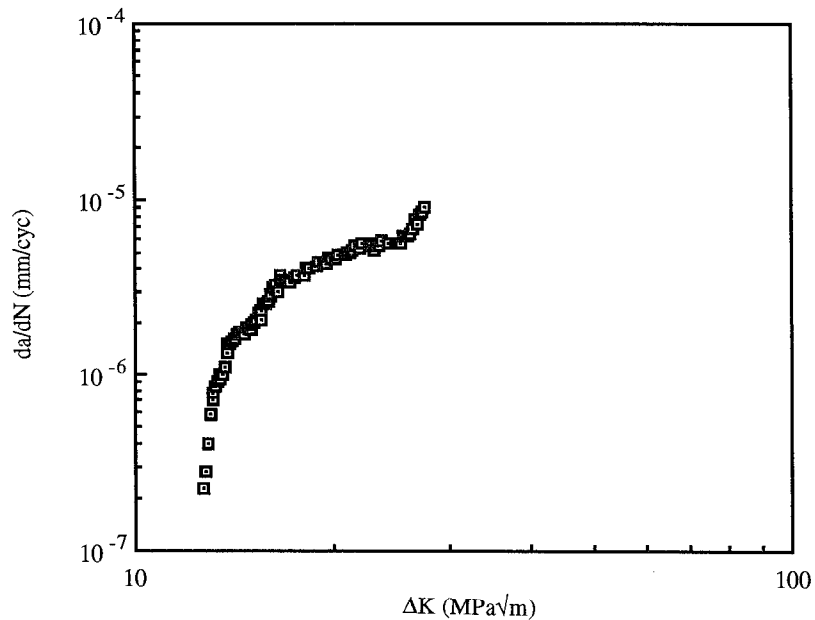


Figure 3. Fatigue crack growth curve (da/dN versus ΔK) for forged IN 718 alloy.

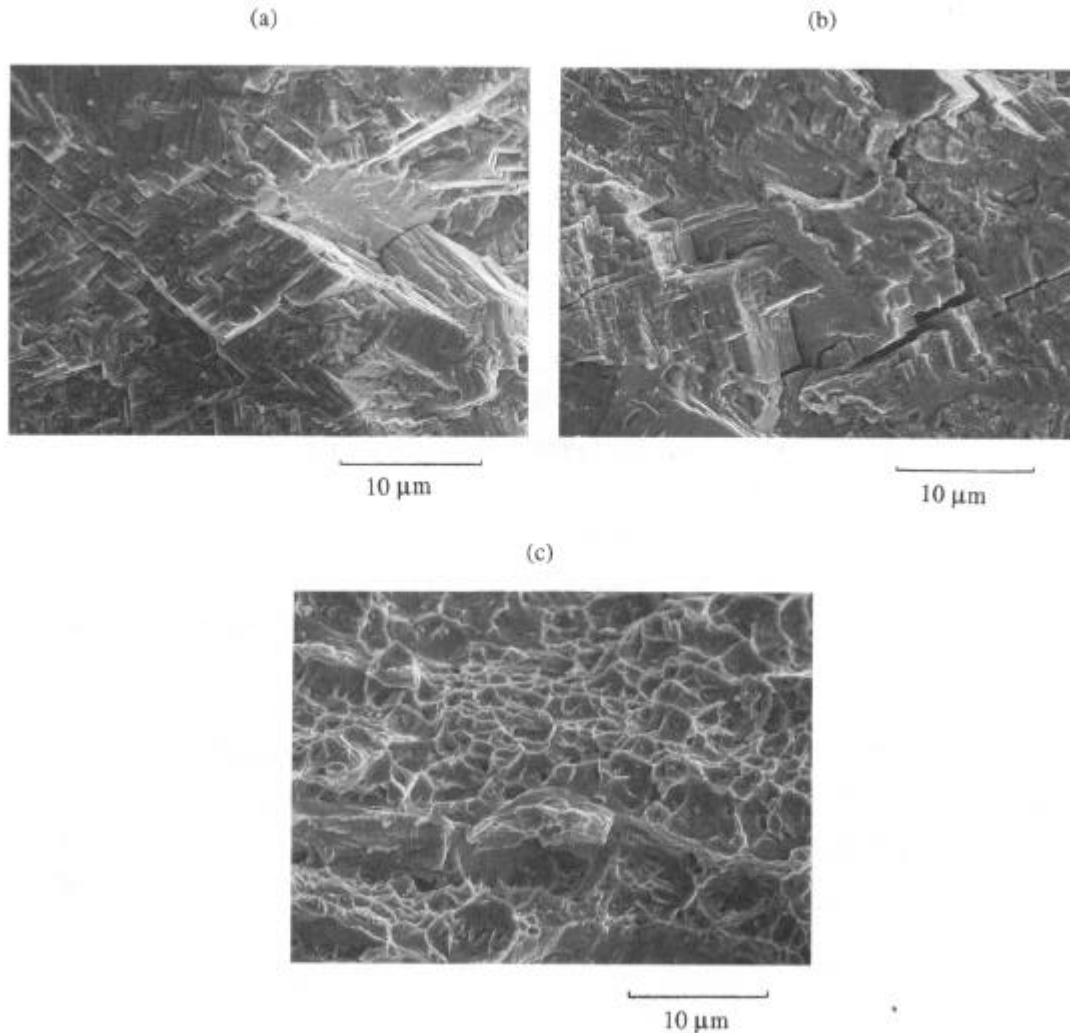


Figure 4. Scanning electron micrographs showing fracture surfaces corresponding to (a) the near-threshold regime and (b) the Paris regime of the fatigue crack growth curve, and (c) the tensile overload region of the specimen.

(iii) Crack-Tip Deformation

The TEM micrographs showing the crack-tip regions for the near-threshold and Paris regimes are presented in Figs. 5 and 6, respectively. No obvious dislocation or twinning activity was observed in either regime and so it appeared that very little plastic deformation was present in the crack-tip regions of these specimens. This is consistent with the SEM fractographic studies discussed above which show a crystallographic fracture mode with no observable plastic deformation. The only deformation feature that was observed in the crack-tip regions of this alloy was shearing of some of the γ' (Ni_3Nb) precipitates. This phenomenon was

observed in both the near-threshold and Paris fatigue crack growth regimes and is illustrated very clearly in Fig. 5 (a) although no evidence of the cutting of these particles by mobile dislocations was present. The sheared portions of the precipitates were not, however, significantly displaced from one another as is often observed following tensile deformation. This was attributed to the partially reversible nature of crack-tip plasticity, causing reversed relative movement of the sheared particle segments and also to the non-ideal orientation of the shearing plane relative to the electron beam direction. The nature of the γ' particle shearing appears to be similar to the shearing γ (Ni_3Al) precipitates reported by Glatzel and Feller-Kniepmeier [4], during fatigue initiation experiments on the alloy CMSX-6. The authors' propose that the mechanism of shearing involves a perfect screw dislocation in the γ matrix dissociating at the γ/γ' interface to produce (i) super partial dislocations in the γ separated by an anti-phase boundary, (APB), or (ii) a super partial dislocation in the γ and a conventional Shockley partial dislocation at the interface, separated by a superlattice intrinsic stacking fault, (SISF). They propose that although the energy of the SISF is higher than that of the APB, the second mechanism may be favored because the partial dislocation formed at the interface will reduce misfit stresses.

It seems likely, therefore, that the mechanism of fatigue crack propagation in this material is by transgranular, crystallographic fracture in favored crystallographic directions induced by the 'unzipping' of atomic bonds directly ahead of the crack-tip. Accommodation of plastic strain ahead of the crack-tip appears to occur via shearing of γ' precipitates presumably by

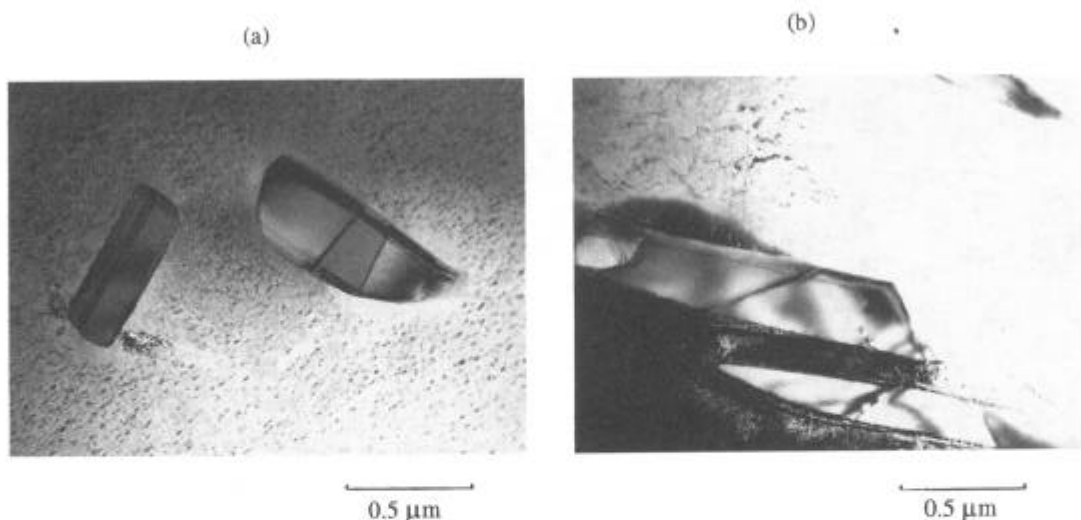


Figure 5. Transmission electron micrographs showing sheared γ' precipitates in crack-tip region corresponding to the near-threshold regime of the fatigue crack growth curve.

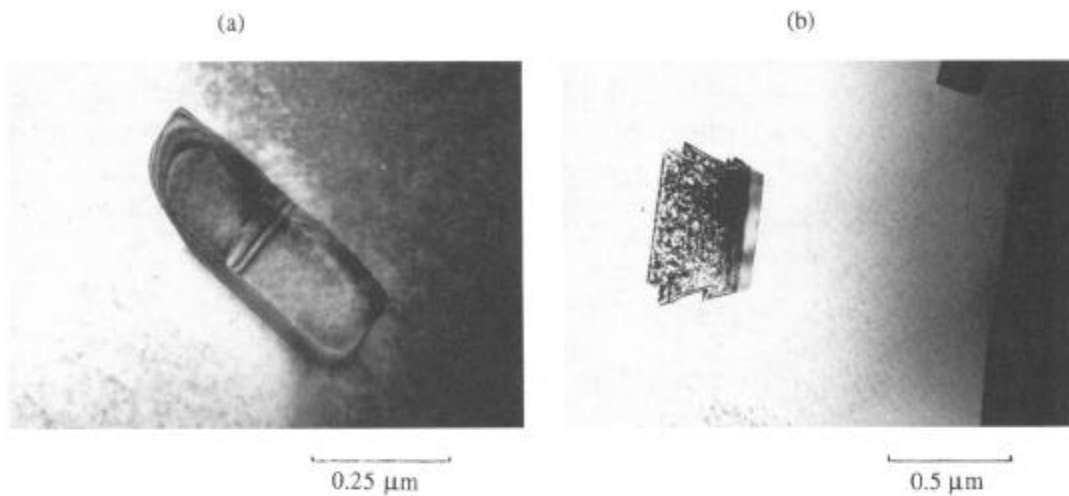


Figure 6. Transmission electron micrographs showing sheared γ' precipitates in crack-tip region corresponding to the Paris regime of the fatigue crack growth curve.

some limited amount of dislocation motion (plastic flow). Also, the fact that there was no observable difference in crack-tip deformation characteristics between the near-threshold and Paris regimes suggests that the mechanism of fatigue crack propagation in this material is independent of ΔK within the range of ΔK that was focused upon in this investigation. A possible change of mechanism to a more classical reversed slip/striation formation mode may occur at a higher ΔK 's than were examined in this study, (i.e. greater than 25 $\text{MPa}\sqrt{\text{m}}$). However, further work is needed to verify this speculation.

4. Summary

1. Stable fatigue crack growth was observed in this alloy between stress intensity factor range values of 13 and 25 $\text{MPa}\sqrt{\text{m}}$. Closer to 13 $\text{MPa}\sqrt{\text{m}}$, a crystallographic fracture mode was observed to occur during fatigue crack growth in this IN 718 alloy. A crystallographic fracture mode was also observed at higher ΔK levels, (close to 25 $\text{MPa}\sqrt{\text{m}}$), along with a significantly higher incidence of secondary cracking.
2. The mechanism of fatigue crack growth in this alloy is by transgranular, crystallographic fracture in favored crystallographic directions induced by the 'unzipping' of atomic bonds directly ahead of the crack-tip. Accommodation of plastic strain ahead of the crack-tip appears to occur via shearing of γ' (Ni_3Al) precipitates and probably a limited amount of dislocation motion (slip).

Acknowledgments

The research is supported by a grant from The Division of Materials Research of The National Science Foundation, with Dr. Bruce MacDonald as Program Monitor. Appreciation is also extended to Dr. Dave Harmon of McDonnell Douglas for the provision of the material that was used in this study.

References

1. J. E. King: *Fatigue of Engineering Materials and Structures*, 1982, Vol. 5, No. 2, pp. 177-188.
2. P. A. S. Reed and J. E. King: *Scripta Metall. Mater.* 1992, Vol. 26, No. 12, pp. 1829-1834.
3. J. E. King: *Materials Science and Technology*, 1987, Vol. 3, No. 9, pp. 750-764.
4. U. Glatzel and M. Feller-Kniepmeier: *Scripta Metall. Mater.* 1991, Vol. 25, No. 8, pp. 1845-1850.
5. D. J. Morrison, V. Chopra and J. W. Jones: *Scripta Metall. Mater.* 1991, Vol. 25, No. 6, pp. 1299-1304.
6. R. Rahouadj, J. Menigault and M. Clavel: *Materials Science and Engineering*, 1987, Vol. 93, pp. 181-190.
7. S. Chen and G. Gottstein: *Journal of Materials Science*, 1989, Vol. 24, No. 11, pp. 4094-4099.
8. D. L. Davidson and K. S. Chan: *Acta Metall.* 1989, Vol. 37, No. 4, pp. 1089-1097.
9. B. A. Lerch and S. D. Antolovich: *Metall. Trans.* 1990, Vol. 21A, No. 8, pp. 2169-2177.
10. S. Suresh: *Fatigue of Materials*, Cambridge University Press, 1991, pp. 202-221.
11. D. P. DeLuca and R. W. Hatala: *Single Crystal PWA 1472*, *ibid*, 1997.